Oxidation modeling of a Si3N4-TiN composite : Comparison between experiment and kinetic models

Frédéric Deschaux-Beaume, Nicole Fréty, Thierry Cutard, Christophe Colin

Oxidation modelling of a Si_3N_4–TiN ceramic: Microstructure and kinetic laws

F. Deschaux-Beaume [a], N. Fréty [b,*], T. Cutard [c], C. Colin [d]

[a] *Université de Montpellier II, LMGC, 34095 Montpellier Cedex 5, France*
[b] *Université de Montpellier II, LPMC, 34095 Montpellier Cedex 5, France*
[c] *Ecole des Mines d'Albi-Carmaux, CROMeP, Campus Jarlard, 81013 Albi Cedex 9, France*
[d] *Ecole Nationale Supérieure des Mines de Paris, Centre des Matériaux P.M. Fourt, 91003 Evry Cedex, France*

Abstract

The oxidation of a silicon nitride–titanium nitride ceramic has been studied. Based on microstructural observations, a phenomenological oxidation model is described, and an oxidation kinetic model has been proposed. For temperatures <1000 °C, only the TiN phase is oxidised. The oxidation process is then controlled by oxygen diffusion through TiO_2, described by a parabolic oxidation kinetic law. The process is more complex above 1000 °C, because of the simultaneous oxidation of both Si_3N_4 and TiN phases. Three oxidation modes, controlled by distinct diffusion mechanisms, take place successively. In a first step, Si_3N_4 and TiN phases are independently oxidised, respectively into SiO_2 and TiO_2 phases. Si_3N_4 oxidation is controlled by oxygen diffusion through SiO_2, while TiN oxidation is controlled by titanium diffusion through TiO_2. In a second step, the TiN oxidation is controlled by oxygen diffusion through TiO_2 and through SiO_2 formed by Si_3N_4 oxidation. In the third step, oxidation of the TiN and Si_3N_4 phases is controlled by oxygen diffusion through the silica layer. Kinetic laws have been proposed for each of these three oxidation modes.

Keywords: B. Microstructure-final; C. Diffusion; D. Nitrides; E. Structural applications

1. Introduction

Silicon nitride based ceramics are good candidates for high-temperature structural applications. With their low-density, low thermal expansion coefficient, high hardness, high-corrosion resistance and high-mechanical resistance, these materials are more appropriate than metals for such applications. However, the development of engineering ceramic components is impeded by the high cost of fine ceramic parts. Electro-conductive ceramics, such as silicon nitride–titanium nitride composites (Si_3N_4–TiN), are of particular interest because they combine the high performance of Si_3N_4-based ceramics with machinability by electro-discharge machining (EDM) [1–3]. In this way, the manufacture cost of ceramic components with complex shapes is limited to the hard metallic material one.

* Corresponding author. Tel.: +33 4 67 14 33 88; fax: +33 4 67 14 42 90.
E-mail address: nfrety@lpmc.univ-montp2.fr (N. Fréty).

However, the main disadvantage of Si_3N_4–TiN ceramics is the oxidation behaviour at high temperatures, which is strongly influenced by the addition of a titanium nitride phase. The oxidation mechanisms of both TiN and Si_3N_4 ceramics have been widely studied and described [4,5]. The oxidation of titanium nitride to rutile (TiO_2) starts between 500 and 600 °C. It is observed that the oxidation is controlled via oxygen diffusion through TiO_2 especially at temperatures <1000 °C [4,6–8]. At higher temperatures, the rate-controlling mechanism is not clearly identified but a cationic diffusion of titanium may be supposed with the outward growth of rutile crystals and the observed porosity under the rutile layer [9,10]. The oxidation of silicon nitride ceramics is also complex [11–17]. Oxidation of pure silicon nitride leads to the formation of a SiO_2 amorphous layer on the surface, separated from the core material by a thin layer of a graded sub-oxide (SiN_xO_y) [18–20] or a crystalline oxynitride (Si_2N_2O) [11–17]. Oxidation is then controlled by the diffusion of oxygen through the SiO_2 and oxynitride layers. Sintered silicon nitride generally oxidises more quickly than pure silicon nitride [21–25]. This is related to

the presence of an intergranular phase originating from sintering additives (Y_2O_3 and Al_2O_3). Some species (Y, Al and O) are more mobile in this phase than in Si_3N_4 at high temperature. Oxidation is then the result of the inward diffusion of oxygen through the oxide layer and the outward diffusion of yttrium and aluminium species through the intergranular phase. Oxidation kinetic, therefore, depends on the composition and amount of the intergranular phase [23].

The oxidation behaviour of Si_3N_4–TiN ceramics is equally complex because the various mechanisms previously presented may act simultaneously. Some studies have been already carried out, but oxidation mechanisms are not yet well understood above 1000 °C [6,26–28]. The aim of the present work is to contribute to the study of the oxidation of Si_3N_4–TiN ceramics, a particular attention being paid to the 1000–1200 °C range. Based on microstructural observations, a phenomenological oxidation modelling is presented as well as the associated kinetic laws.

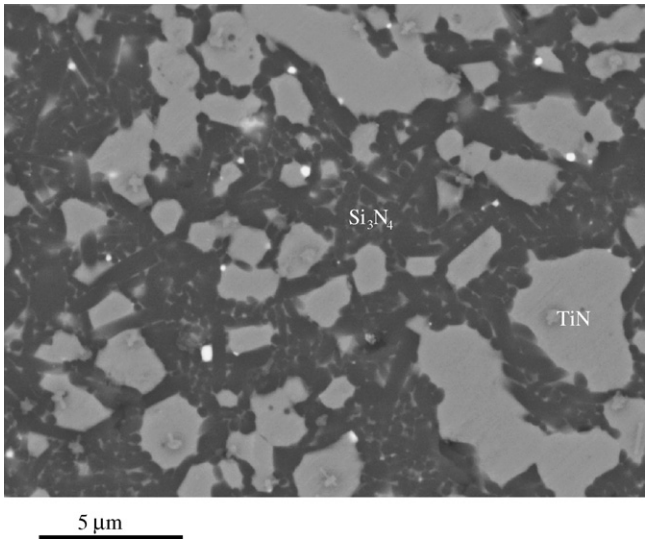

Fig. 1. Microstructure of the silicon nitride–titanium nitride ceramic.

2. Experimental procedure

The studied material is a commercial ceramic (KERSIT 601, Norton Desmarquest, FR), prepared by sintering from a mixture of Si_3N_4 and TiN powders in equivalent ponderal proportions. A few percent of high purity Y_2O_3 and Al_2O_3 powders is added to the initial mixture. The size distribution and the proportion of TiN particles (50 wt.%, i.e. 30 vol.%) have been chosen to confer to the material a sufficient electrical conductivity for electro-discharge machining, without significant decrease of mechanical characteristics [2]. In this way, the ceramic microstructure consists of a continuous TiN network, surrounded by a Si_3N_4 based matrix, containing a fine SiYAlON intergranular phase (Fig. 1).

Parallelepipedic samples (10 mm × 4 mm × 2 mm) were machined using electro-discharge machining, then polished with diamond pastes down to the 1 µm grade. Samples were oxidised at 1150 °C in air for 1–200 h. The microstructure of the sound and oxidised materials was characterised by scanning electron microscopy (SEM) (Zeiss, DSM982 Gemini). Complementary analyses were performed by energy dispersive spectrometry (EDS) (Noran, Voyager IV) and wavelength-dispersive spectrometry (WDS) (Cameca Instruments, SX 50).

3. Phenomenological oxidation modelling

3.1. Microstructural investigations

Microstructural observations were investigated on the TiN–Si_3N_4 material, which was oxidised at 1150 °C in air for a duration of 1–200 h. For oxidation duration of 100 h, a 50 µm thick oxidised area is observed on the polished cross section in which large microstructural modifications have taken place (Fig. 2). The morphology of this oxidised area is similar to that observed by Bellosi et al. [6] and by Gogotsi et al. [26,28] on similar materials. Three layers are distinguishable in this area from the surface to the non-

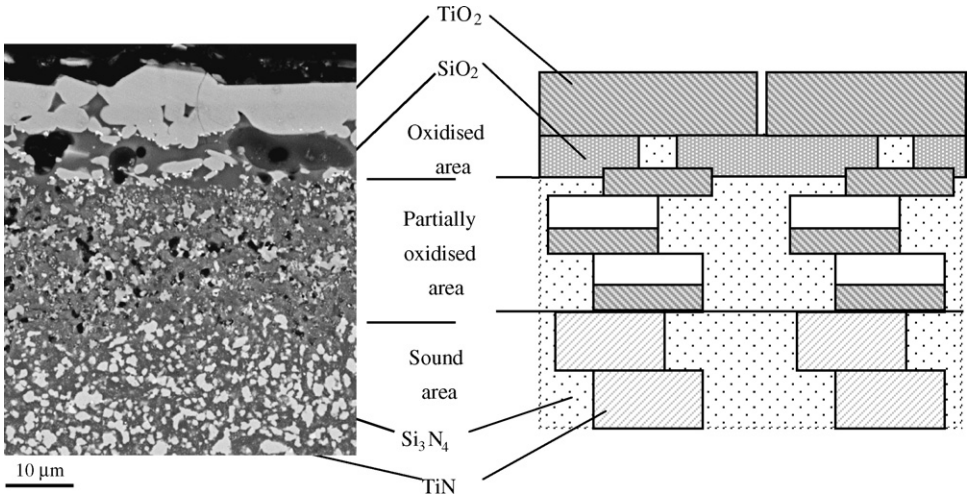

Fig. 2. SEM image and schematic representation of the Si_3N_4–TiN ceramic surface after oxidation of 100 h at 1150 °C.

oxidised material core. The first layer (layer 1) is composed primarily of large crystals, which were identified as a TiO_2 phase, according to the WDS analysis. The second layer (layer 2) is composed of isolated TiO_2 crystals and a continuous glassy phase. This phase, the composition of which being close to the stoichiometric SiO_2, results from the Si_3N_4 oxidation. Small grains, which are aluminium- and/or yttrium-rich phases are observed in this second layer. This indicates the diffusion of aluminium toward the surface as previously observed in the case of the oxidation of Si_3N_4 ceramics with an intergranular glassy phase. Large pores with diameters of 2–20 μm are also observed. The third layer (layer 3) exhibits a more complex microstructure consisting of several phases (SiO_2, TiO_2, Si_3N_4, TiN) and porosity.

The evolution of the morphology of the oxidised surface was studied according to the oxidation duration [29]. The diffusion of titanium toward the surface occurs very rapidly at 1150 °C, as is shown by the continuous TiO_2 surface layer and the sub-layer porosity, already formed after 1 h of oxidation. The growth of the surface layer (layer 1) is rapid at the beginning of oxidation. It then slows down to reach a thickness of 5–10 μm after 10 h, which remains constant. For oxidation times >50 h, the TiO_2 surface layer contains numerous cracks. After about 100 h of oxidation, a continuous layer of SiO_2 containing large cavities starts forming under and around the surface TiO_2 crystals.

3.2. Oxidation phenomenological modelling

According to the microstructural investigations, and literature data concerning oxidation controlling mechanisms in Si_3N_4 and TiN materials, a phenomenological model has been developed to describe the oxidation of the studied Si_3N_4–TiN ceramic, in the 1000–1200 °C temperature range. The proposed model consists in three steps, where the oxidation of both TiN and Si_3N_4 phases is controlled by one or several diffusion mechanisms (Fig. 2):

(i) *First step*.

In the first step, the oxidation of the TiN phase involves the formation of a rutile (TiO_2) layer at the outer surface of the TiN particles, according to the reaction (1):

$$TiN(s) + O_2(g) \leftrightarrow TiO_2(s) + \tfrac{1}{2}N_2(g) \quad (1)$$

It is generally admitted that TiN oxidation is controlled by the diffusion of oxygen through TiO_2 [16,27]. However the diffusion of Ti can be faster above 1000 °C or within monocrystalline TiO_2 [16,30]. During this step, the TiN oxidation is controlled by the diffusion of Ti through TiO_2, leading to the growth of the surface rutile crystals. This outward diffusion creates vacancies in the TiN network, which can coalesce to form closed porosity. The Si_3N_4 oxidation in mainly vitreous silica (SiO_2) takes place at the same time, and is controlled by oxygen diffusion through SiO_2 (2):

$$Si_3N_4(s) + 3O_2(g) \leftrightarrow 3SiO_2(s) + 2N_2(g) \quad (2)$$

However, this mechanism is slower than TiN oxidation one. The porosity created in the outer TiN particles reduces the surface available for Ti diffusion and leads to a slow-down of the titanium diffusion towards the free surface. On the other hand, oxygen can cross this closed porosity in a molecular form.

(ii) *Second step*.

In the second step, oxygen diffuses faster than titanium through the surface TiO_2 crystals and oxidises inner TiN particles. The transformation of Si_3N_4 into SiO_2, controlled by the same mechanism than in the first step, leads to a great molar volume increase (+96%). The stresses induced by this volume change may be relaxed by creep of SiO_2 in the sub-layer porosity [31]. This vitreous phase flows into the porosity resulting from the titanium diffusion, and progressively fills in the sub-layer, forming a continuous layer. The diffusion of oxygen through SiO_2 being slower than through TiO_2, the progressive filling of the porosity with SiO_2 leads to a decrease of the diffusion rate of oxygen towards inner TiN phase.

(iii) *Third step*.

In the third step, for longer oxidation duration, the oxidation process is controlled by a single mechanism, which is the diffusion of oxygen through a dense SiO_2 layer. The SiO_2 phase forms a continuous layer below the large surface TiO_2 crystals. Oxygen then diffuses through this layer to oxidise both Si_3N_4 and TiN phases. The third step is then a stationary oxidation mode, reached after two transient modes.

4. Oxidation kinetic laws

4.1. Simplifying assumptions

In order to obtain relatively simple kinetic laws, some simplifying assumptions have to be done. First, diffusion is considered to be unidirectional through each material phase, from the surface to the bulk or inversely. Secondly, it is assumed that the TiN particles distribution is homogeneous in the sound material. That involves proportions of TiN and Si_3N_4 phases are constant on each section of the sound material parallel to the surface.

4.2. Oxidation kinetic laws below 1000 °C

Silicon nitride oxidation is very slow at temperatures <1000 °C [16]. Up to this temperature, only the TiN phase in the material is significantly oxidised in rutile (TiO_2), and the total mass gain measured, Δm, corresponds to the mass gain of the TiN phase, Δm_{TiN} (3):

$$\frac{\Delta m}{S} = \frac{\Delta m_{TiN}}{S} = \frac{\Delta m_{TiN}}{S_{TiN}} \frac{S_{TiN}}{S} \quad (3)$$

where S is the total outer surface of the sample, and S_{TiN} is the outer surface of the TiN phase.

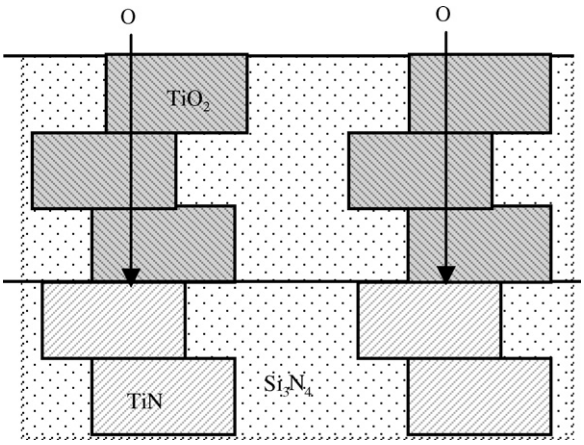

Fig. 3. Oxidation mechanism of the Si_3N_4–TiN material for temperature <1000 °C.

It is generally admitted that oxidation of Ti and TiN is controlled by oxygen diffusion, which is faster than Ti diffusion in polycrystalline TiO_2 below 900 °C (Fig. 3) [4,7–10,30,32]. Fig. 4 shows the morphology of the surface of the material oxidised for 100 h at 800 °C, in which the TiN surface grains are replaced by TiO_2 ones. Up to 900 °C, the isothermal oxidation kinetic is then given by a parabolic law (4):

$$\frac{\Delta m}{S} = \frac{S_{\mathrm{TiN}}}{S} k_{\mathrm{P_{O/TiO_2}}}^{1/2} t^{1/2} + \frac{\Delta m_{0_{\mathrm{TiN}}}}{S} \tag{4}$$

where $k_{\mathrm{P_{O/TiO_2}}}$ is the parabolic rate constant corresponding to TiN oxidation below 900 °C (controlled by O diffusion through TiO_2), t is the oxidation time, and $\Delta m_{0_{\mathrm{TiN}}}$ is the mass gain at the beginning of the parabolic oxidation mode.

A transition takes place between 900 and 1000 °C, due to two phenomena: the beginning of oxidation of the Si_3N_4 phase, and the change in mechanism controlling oxidation of the TiN phase in the ceramic. Below 900 °C, this mechanism is oxygen diffusion through TiO_2, whereas above 1000 °C, it is titanium diffusion, as showed by the continuous TiO_2 layer formed in the ceramic surface (Fig. 5) and the porosity in the sub-layer (Fig. 2). This mechanism change is due to the higher activation energy of titanium diffusion through TiO_2 or to the growth of TiO_2 crystals in the ceramic surface, which reduces the number of grain boundaries, and then the short circuit diffusion paths for oxygen. Indeed, it is admitted that oxygen diffusion is faster than titanium diffusion in polycrystalline TiO_2, due to grain boundary diffusion paths, whereas the diffusion mechanism is different for monocrystalline TiO_2 [4,30].

4.3. Oxidation kinetic laws between 1000 and 1200 °C

Oxidation mechanisms are more complex above 1000 °C, because of the simultaneous oxidation of both TiN and Si_3N_4 phases as previously described and represented on Fig. 6. The total mass gain per unit area can then be expressed as a function of TiN and Si_3N_4 mass gains according to the relation (5):

$$\frac{\Delta m}{S} = \frac{\Delta m_{\mathrm{TiN}} + \Delta m_{\mathrm{Si_3N_4}}}{S} \tag{5}$$

where Δm, Δm_{TiN} and $\Delta m_{\mathrm{Si_3N_4}}$, are respectively, the mass gains of the material, the TiN phase and the Si_3N_4 phase, and S is the outer surface of the sample.

(i) *Oxidation kinetic law of Si_3N_4.*

The oxidation of silicon nitride phase is controlled by oxygen diffusion through silica. The incremental mass gain for this phase, resulting from an isothermal oxidation of duration dt can be expressed according to relation (6):

$$\mathrm{d}\left(\frac{\Delta m_{\mathrm{Si_3N_4}}}{S}\right) = \frac{1}{2} k_{\mathrm{P_{O/SiO_2}}}^{1/2} \frac{S_{\mathrm{Si_3N_4}}}{S} t^{-1/2}\,\mathrm{d}t \tag{6}$$

where $k_{\mathrm{P_{O/SiO_2}}}$ is the parabolic rate constant corresponding to the Si_3N_4 oxidation, and $S_{\mathrm{Si_3N_4}}$ is the outer surface of the silicon nitride phase.

(ii) *Oxidation kinetic law of TiN.*

The oxidation of TiN phase is more complex, and kinetic depends on the oxidation stage.

During the first stage (first transient oxidation mode) above 1000 °C, the rate of titanium diffusion through TiO_2 overlapping the surface of TiN network is greater than the oxygen

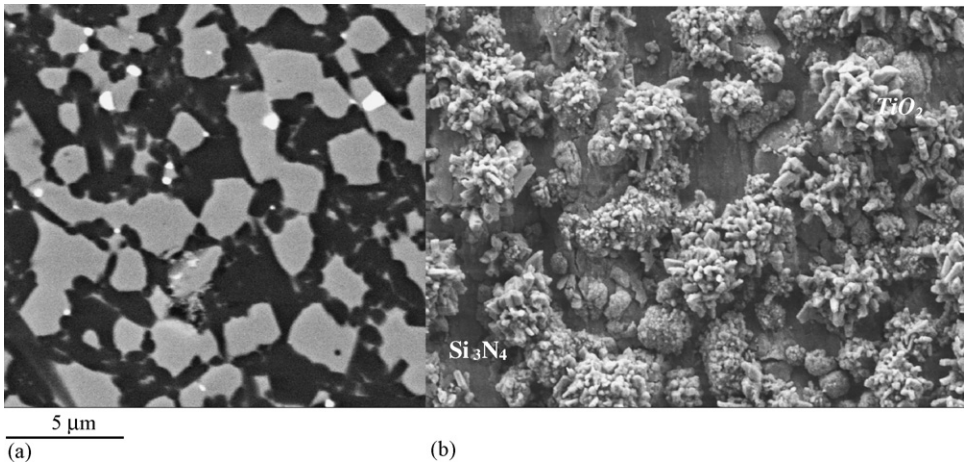

Fig. 4. Microstructure of the Si_3N_4–TiN material surface (a) sound material and (b) material after oxidation at 800 °C during 100 h.

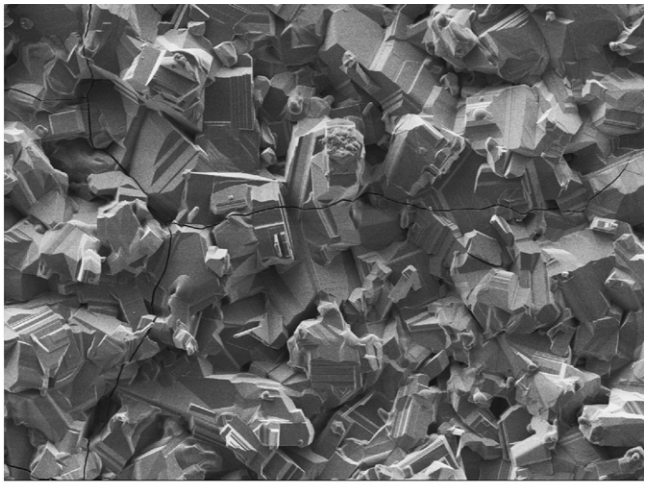

Fig. 5. Microstructure of the Si_3N_4–TiN material surface after oxidation at 1150 °C during 100 h.

diffusion one. The TiN oxidation kinetic is thus controlled by the diffusion of titanium towards the free surface, characterised by the parabolic rate constant $k_{P_{Ti/TiO_2}}$, and the available surface S_{Ti/TiO_2} (surface between TiO_2 and inner TiN particles). The incremental mass gain for oxidation of TiN phase during dt is then given by relation (7a):

$$\mathrm{d}\left(\frac{\Delta m_{TiN}}{S}\right) = \frac{1}{2} k_{P_{Ti/TiO_2}}^{1/2} \frac{S_{Ti/TiO_2}}{S} t^{-1/2}\,\mathrm{d}t \tag{7a}$$

The titanium diffusion towards the free surface creates porosity within the TiN network, close to the TiN/TiO_2 interface, which leads to a decrease of the surface S_{Ti/TiO_2}, and of the average diffusion rate of titanium, expressed by the $(k_{P_{Ti/TiO_2}}^{1/2} S_{Ti/TiO_2}/S)$term.

In a first approximation, the variation of the diffusion surface during dt, dS_{Ti/TiO_2}, is proportional to S_{Ti/TiO_2} and to the quantity of formed TiO_2. This quantity can be expressed by the average thickness variation of the TiO_2 layer, dx [33]:

$$-\mathrm{d}S_{Ti/TiO_2} = C_1 S_{Ti/TiO_2}\,\mathrm{d}x \tag{8}$$

where C_1 is a constant.

Integrating relation (8), the following expression is obtained:

$$S_{Ti/TiO_2} = C_2 \exp(-C_1 x) \tag{9}$$

where C_2 is a constant.

The growth of the TiO_2 surface layer being controlled by the titanium diffusion through TiO_2 during the first mode, the x variation at the time t can be written according to relation (10):

$$\frac{\mathrm{d}x}{\mathrm{d}t} = \frac{1}{2} k^{1/2} \frac{S_{Ti/TiO_2}}{S} t^{-1/2} \tag{10}$$

where k is deduced from the parabolic rate constant $k_{P_{Ti/TiO_2}}$ (11):

$$k = k_{P_{Ti/TiO_2}} \left(\frac{1 + M_{Ti}/2M_O}{1 - M_N/2M_O}\right) \frac{1}{\rho_{TiO_2}^2} \tag{11}$$

with ρ_{TiO_2} the TiO_2 density, and M_{Ti}, M_O and M_N the molar masses of Ti, O and N. Replacing S_{Ti/TiO_2} by expression (9) in Eq. (10), the following relations are obtained:

$$x = \frac{1}{C_1} \ln(at^{1/2} + 1) \quad (\text{with the assumption } x = 0 \text{ at } t = 0) \tag{12}$$

and

$$S_{Ti/TiO_2} = C_2 \left(\frac{1}{at^{1/2} + 1}\right) \tag{13}$$

with $a = k^{1/2} C_1 C_2/S$, constant at a fixed temperature, and $C_2 = S_{TiN}$ (initial outer surface of the TiN phase). The $S_{TiN/S}$ ratio is equal to the volume proportion of the TiN phase in the material. This quantity was determined by image analysis, and is equal to 0.3 (and $S_{Si_3N_4}/S = 0.7$).

The first transient mode acts while the titanium diffusion towards the free surface is faster than the oxygen diffusion towards the inner TiN particles. Oxygen diffuses through the formed porosity in a molecular form, and its rate diffusion is not significantly changed with the S_{Ti/TiO_2} evolution if it is assumed that oxygen diffusion in porosity is faster than in TiO_2.

During the second stage (second transient oxidation mode), TiN oxidation is controlled by the diffusion of oxygen towards inner TiN particles. Si_3N_4 oxidation in mainly SiO_2 takes place with an important molar volume increase. Silica gradually fills

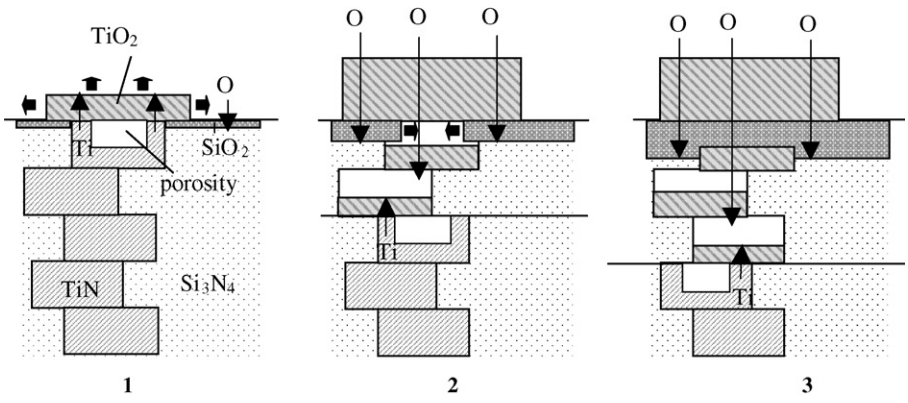

Fig. 6. The three steps of the oxidation model for temperature >1000 °C.

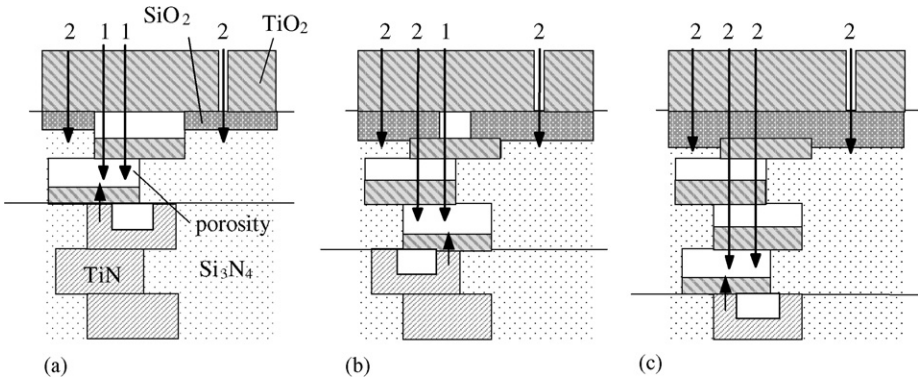

Fig. 7. Evolution of oxidation mechanisms during the second oxidation mode.

the porous sub-layer. The TiN oxidation kinetic is controlled, during this mode, by two simultaneous mechanisms (Fig. 7): the diffusion of oxygen through TiO_2, characterised by the rate constant $k_{p_{O/TiO_2}}$ (mechanism 1), and the diffusion of oxygen through silica (which is slower than through TiO_2), characterised by the rate constant $k_{p_{O/SiO_2}}$ (mechanism 2). The incremental mass gain during dt is given by the following Eq. (7b):

$$\mathrm{d}\left(\frac{\Delta m_{TiN}}{S}\right) = \frac{1}{2}\left(k^{1/2}_{p_{O/TiO_2}}\frac{S_{O/TiO_2}}{S} + k^{1/2}_{p_{O/SiO_2}}\frac{S_{SiO_2/TiO_2}}{S}\right)t^{-1/2}\,\mathrm{d}t \tag{7b}$$

where S_{O/TiO_2} and S_{SiO_2/TiO_2} are the available surfaces for oxygen diffusion towards inner TiN particles related to each mechanism.

The transition time, t_1, between the first and second transient modes then corresponds to the equality:

$$k^{1/2}_{p_{Ti/TiO_2}} S_{Ti/TiO_2}(t_1) = k^{1/2}_{p_{O/TiO_2}} S_{O/TiO_2}(t_1) + k^{1/2}_{p_{O/SiO_2}} S_{SiO_2/TiO_2}(t_1) \tag{14}$$

During oxidation above 1000 °C, the S_{SiO_2/TiO_2} contact surface between SiO_2 and inner TiO_2 phases increases up to S_{TiN}, while the S_{O/TiO_2} contact surface between oxygen from outer porosity and inner TiO_2 phase decreases down to zero (Fig. 7), with respect to the equality (15):

$$S_{SiO_2/TiO_2} + S_{O/TiO_2} = S_{TiN} \tag{15}$$

Assuming that SiO_2 creeps rapidly at the considered temperature (instantaneous stress relaxation), the variation of surface overlapped by SiO_2 during dt, dS_{SiO_2} (with $S_{SiO_2} = S_{SiO_2/TiO_2} + S_{Si_3N_4}$, see Fig. 7), is proportional to the quantity of oxygen having replaced nitrogen in the Si_3N_4 phase to form silica [18,19,29], i.e. to the variation of the quantity of formed silica:

$$\mathrm{d}S_{SiO_2} = A_1 S_{Si_3N_4}\,\mathrm{d}y \tag{16}$$

where A_1 is a constant and dy is the thickness variation of the SiO_2 layer during dt.

The quantity of formed SiO_2 is diffusion controlled, so in an early approximation, S_{SiO_2} is given by relation (17):

$$S_{SiO_2} = S_{Si_3N_4}(1 + bt^{1/2}) \quad \text{while} \quad S_{SiO_2} \le S \tag{17}$$

with

$$b = \frac{A_1 k^{1/2}_{p_{O/SiO_2}}}{\rho_{SiO_2}}\left(\frac{1 + M_{Si}/2M_O}{1 - 2M_N/3M_O}\right), \tag{18}$$

constant at a fixed temperature

and

$$\frac{S_{O/TiO_2}}{S} = 1 - \frac{S_{SiO_2}}{S} \tag{19}$$

In the third stage (stationary mode), when the whole sub-layer is filled with SiO_2 ($S_{SiO_2} = S$), TiN oxidation is controlled by oxygen diffusion through SiO_2, and the incremental mass gain of the TiN phase is expressed according to the relation (7c):

$$\mathrm{d}\left(\frac{\Delta m_{TiN}}{S}\right) = \frac{1}{2}k^{1/2}_{p_{O/SiO_2}}\frac{S_{TiN}}{S}t^{-1/2}\,\mathrm{d}t \tag{7c}$$

The oxidation behaviour of the silicon nitride–titanium nitride composite for temperatures >1000 °C is then described by the following kinetic laws for each mode of the oxidation mechanism:

- if $0 \le t \le t_1$ (first mode), where t_1 is obtained according to the Eq. (14):

$$\frac{\Delta m}{S} = \frac{0.3}{a}k^{1/2}_{p_{Ti/TiO_2}}\ln(at^{1/2} + 1) + 0.7k^{1/2}_{p_{O/SiO_2}}t^{1/2} + \frac{\Delta m_0}{S} \tag{20a}$$

$$\frac{\Delta m}{S} = (0.3k^{1/2}_{p_{O/TiO_2}} + 0.7k^{1/2}_{p_{O/SiO_2}})t^{1/2} + \frac{0.7}{2}(k^{1/2}_{p_{O/SiO_2}} - k^{1/2}_{p_{O/TiO_2}})bt + \frac{\Delta m'_0}{S} \tag{20b}$$

- if $t_1 \le t \le t_2$ (second mode), with $S_{SiO_2}(t_2) = S$
- if $t \ge t_2$ (third mode)

$$\frac{\Delta m}{S} = k^{1/2}_{p_{O/SiO_2}}t^{1/2} + \frac{\Delta m''_0}{S} \tag{20c}$$

where Δm_0, $\Delta m'_0$ and $\Delta m''_0$ are constants.

5. Discussion

5.1. Evolution of kinetic parameters of TiN phase oxidation, at a fixed temperature

Oxidation rate of Si_3N_4 phase is controlled by a single parameter (Eq. (6)), whereas the rate controlling parameter for TiN phase oxidation changes with the oxidation mode (Eqs. (7a)–(7c)). Fig. 8 presents a typical evolution of the kinetic parameters characterising the TiN phase oxidation at a fixed temperature, during the two first oxidation modes. The parabolic rate constants, and other kinetic constants were chosen according to bibliographical data, with respect to the condition $k_{P_{Ti/TiO_2}} > k_{P_{O/TiO_2}} \gg k_{P_{O/SiO_2}}$ [4,6,30,34].

Two competitive mechanisms are responsible for the TiN oxidation: Titanium diffusion through TiO_2 towards the surface, controlled by a first kinetic parameter (Eq. (7a)), and oxygen diffusion through TiO_2 and/or SiO_2 towards inner TiN particles, controlled by a second kinetic parameter (Eq. (7b)). The oxidation is controlled by the faster mechanism, i.e. the mechanism having the greater kinetic parameter. At the first oxidation stage, the kinetic parameter corresponding to titanium diffusion is higher than the oxygen diffusion one, then oxidation is controlled by titanium diffusion. The first kinetic parameter decreases with oxidation time, due to the porosity formation. In the same time, the second kinetic parameter, controlling oxygen diffusion, decreases too, due to the formation of SiO_2, which creeps into porosity. But the decrease of the second parameter being slower than the first one, the gap between the two parameters is progressively reduced. When the kinetic parameter corresponding to the oxygen diffusion is equal to the titanium diffusion one, after an oxidation time t_1 (Eq. (14)), the oxidation process becomes controlled by oxygen diffusion. This new stage corresponds to the second oxidation mode. During this stage, the two kinetic parameters have the same value, the decrease of the Ti diffusion parameter being controlled by the decrease rate of the oxygen diffusion parameter. This parameter keeps decreasing throughout the second mode, with the growth and creep of SiO_2 phase into porosity. It finally stabilises after a time t_2, when SiO_2 overlaps the whole sub-layer, and its value remains constant during the third mode.

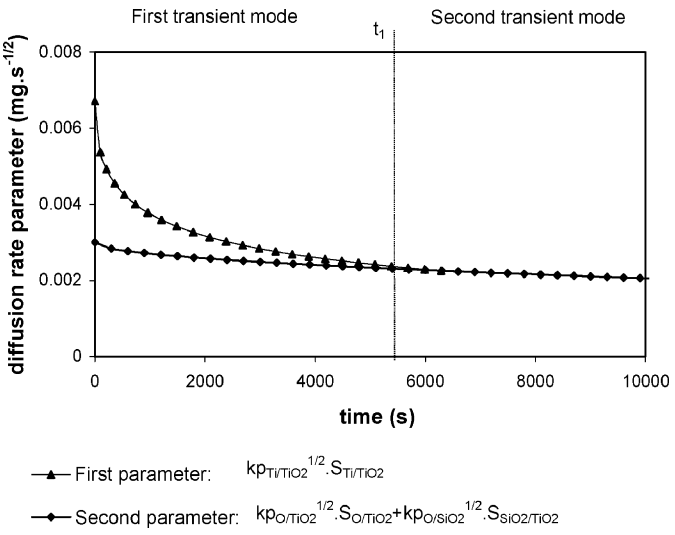

Fig. 8. Variation of oxidation kinetic parameters of the TiN phase with time ($k_{P_{Ti/TiO_2}} = 5.10^{-4}\,mg^2\,s^{-1}$, $k_{P_{O/TiO_2}} = 10^{-4}\,mg^2\,s^{-1}$, $k_{P_{O_2/SiO_2}} = 10^{-6}\,mg^2\,s^{-1}$, $a = 0.025$ and $b = 0.0015$).

5.2. Temperature dependence of the mode time limits

The three oxidation modes are divided by time limits (t_1 and t_2), depending on temperature. The evolution trend of these limits was studied, for temperature variation in the 1000–1200 °C range.

The variation of mode time limits is due to the fact that parabolic rate constants depend on temperature. Those constants correspond to each elementary diffusional mechanism involved in the oxidation process:

$$k_{P_{Ti/TiO_2}} = k_{0_1} \exp\left(-\frac{E_{a_1}}{RT}\right) \tag{21a}$$

$$k_{P_{O/TiO_2}} = k_{0_2} \exp\left(-\frac{E_{a_2}}{RT}\right) \tag{21b}$$

$$k_{P_{O/SiO_2}} = k_{0_3} \exp\left(-\frac{E_{a_3}}{RT}\right) \tag{21c}$$

where E_{a_i} are the activation energies of each diffusional mechanism, and k_{0_i} are direct ratio constants.

In order to evaluate the effect of the temperature variation on the mode time limits, characteristic parameters of these equations have been chosen, according to literature data [4,6,16,34]. The evolution of the parabolic rate constants with temperature, for the chosen parameters, is reported in Fig. 9. In agreement with the oxidation model, the parabolic constant for titanium diffusion is higher than the oxygen diffusion one in TiO_2, which is higher than the oxygen diffusion one in SiO_2, in the whole considered temperature range (1000–1200 °C). The values of the constants $k_{P_{Ti/TiO_2}}$ and $k_{P_{O/TiO_2}}$ are of about the same magnitude order, whereas $k_{P_{O_2/SiO_2}}$ is very lower, especially in the lowest temperature range. When temperature increases, the gap

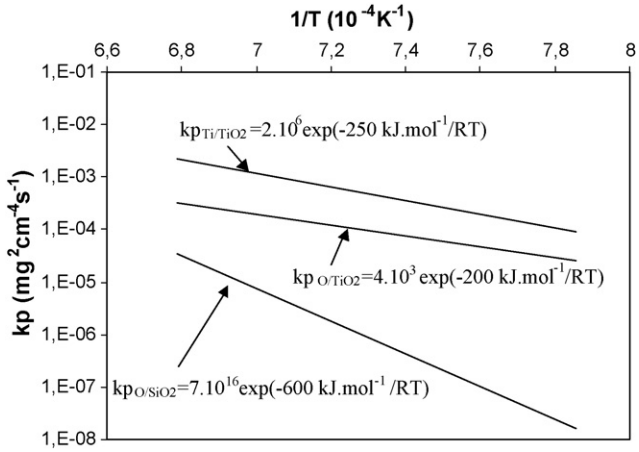

Fig. 9. Evolution of parabolic rate constants of the three diffusional mechanisms vs. temperature.

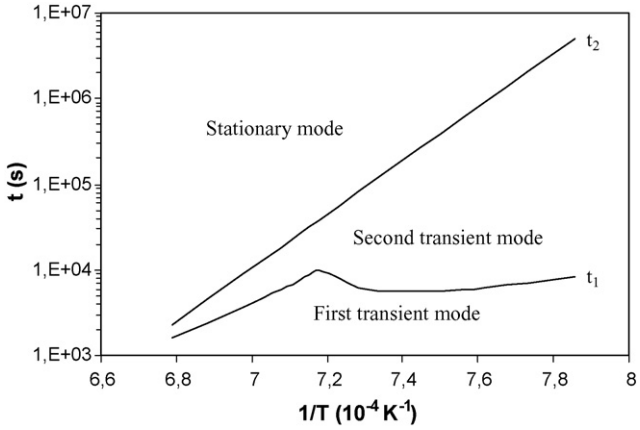

Fig. 10. Evolution of the time limits, t_1 and t_2, of the two transient modes vs. temperature.

between $k_{P_{Ti/TiO_2}}$ and $k_{P_{O/TiO_2}}$ increases slightly, whereas the gap between $k_{P_{O/SiO_2}}$ and other parabolic constants decreases rapidly.

The time t_1, separating the first and second transient modes, is obtained solving Eq. (14), which expresses the equality between the two kinetic parameters of Fig. 8. The solution is a very complex linear combination of $k_{P_{Ti/TiO_2}}$, $k_{P_{O/TiO_2}}$ and $k_{P_{O/SiO_2}}$, so its variation with temperature depends on the three activation energies E_{a_1}, E_{a_2} and E_{a_3}. The t_1 evolution is represented in Fig. 10. For the lowest temperature range, a weak variation of t_1 is observed. But for higher temperature, t_1 decreases rapidly when the temperature increases.

This complex evolution may be explained considering Eq. (14) and Fig. 8. When the temperature increases, the gap between the diffusion rates of titanium and oxygen in TiO_2 also increases $(E_{a_1} > E_{a_2})$, so the gap between the kinetic parameters of the two competitive mechanisms is greater at the beginning of oxidation (Fig. 8). The temperature increase also leads to the activation of the SiO_2 formation, which reduces the oxygen diffusion rate towards inner TiN particles, so it accelerates the decrease of the second kinetic parameter. These first effects tend to increase the transitory time t_1. But the temperature increase reduces also the gap between oxygen diffusion rate through TiO_2 and SiO_2 $(E_{a_3} > E_{a_2})$, and then limits the decrease of the second kinetic parameter. On another way, the decrease of the first parameter is accelerated. Then, these second effects tend to decrease the transitory time t_1. The t_1 evolution with temperature (Fig. 10) may then be explained considering these two opposite effects: at the lower temperatures, the two effects are compensated each other, so t_1 variation is low and at higher temperature, the second effect becomes predominant, and t_1 decreases rapidly.

The third oxidation mode begins when a sufficient quantity of silica is formed to cover the whole outer surface of the material ($S_{SiO_2} = S$ in Eq. (17)). Then time t_2 is controlled only by oxygen diffusion rate through silica, and is expressed by the relation:

$$t_2 = A_2 \exp\left(\frac{E_{a_3}}{RT}\right) \tag{22}$$

where A_2 is a constant.

6. Conclusion

The oxidation behaviour of silicon nitride–titanium nitride is studied in this paper, specially in the 1000–1200 °C temperature range. Based on microstructural investigations, an oxidation model has been proposed. This oxidation model consists of three successive modes. First Si_3N_4 and TiN phases are independently oxidised, respectively into SiO_2 and TiO_2 phases. Si_3N_4 oxidation is controlled by oxygen diffusion through SiO_2, while TiN oxidation is controlled by titanium diffusion through TiO_2. The titanium depletion involves the creation of porosity between TiN and TiO_2, which reduces the oxidation rate of the TiN phase. Secondly, when titanium diffusion rate is too low, oxygen diffuses towards inner TiN particles. The TiN oxidation is then controlled by oxygen diffusion through TiO_2 and through SiO_2 formed by Si_3N_4 oxidation, which progressively fills porosity of the material sub-layer. Thirdly, when SiO_2 forms an amorphous continuous layer under the TiO_2 surface layer, oxidation of the TiN and Si_3N_4 phases is controlled by oxygen diffusion through this silica layer.

Kinetic laws have been proposed for each of these three oxidation modes. Both phases forming a continuous network, oxidation kinetics of each phase may be considered independently. Si_3N_4 oxidation is controlled, during the whole process, by oxygen diffusion through silica, the oxidation kinetic law being then parabolic. TiN oxidation is the result of two opposite diffusional mechanisms: titanium diffusion through TiO_2 towards the surface, and oxygen diffusion through TiO_2 and/or SiO_2 towards inner TiN particles. During the first mode, kinetic parameters of the first mechanism is higher than the ones of the second mechanism, and TiN oxidation is controlled by titanium diffusion. Both kinetic parameters decrease during the two first modes, but the decrease rate of the second one is slower than the first one. When both parameters are equal, TiN oxidation becomes controlled by oxygen diffusion (second mode). The kinetic parameter controlling this mechanism decreases again, until SiO_2 overlaps the whole sub-layer, and oxidation kinetic of TiN becomes parabolic (third mode). The time limits of these modes are temperature dependent, and have been expressed according to the activation energy of the different diffusional mechanisms taking place during oxidation process.

References

[1] M. Higuchi, M. Miyake, H. Kakeuchi, E. Kamjo, Electrically conductive sintered compact of Si_3N_4 machinable by electrical discharge machinable and process of producing the same, US Patent 4 659 508, 1987.

[2] C. Martin, P. Mathieu, B. Cales, Electrical discharge machinable ceramic composites, in: R.J. Brook (Ed.), Proceedings of Symposium on Ceramic Materials Research, E-MRS Spring Conference, Strasbourg (France), 1988.

[3] A. Bellosi, S. Guicciardi, A. Tampieri, Development and characterization of electroconductive Si_3N_4–TiN composites, J. Eur. Ceram. Soc. 9 (1992) 83–93.

[4] J. Desmaison, P. Lefort, M. Billy, Oxidation mechanism of titanium nitride in oxygen, Oxid. Met. 13 (6) (1979) 505–517.

[5] M. Billy, Reactivity in nitrogen ceramics, in: Proceedings of the Science of Ceramics14th International Conference, Stoke-on-Trent (UK), The Institute of Ceramics, 1987, pp. 45–60.

[6] A. Bellosi, A. Tampieri, Y.Z. Liu, Oxidation behaviour of electroconductive Si_3N_4–TiN composites, Mater. Sci. Eng. A127 (1990) 115–122.
[7] A. Tampieri, E. Landi, A. Bellosi, The oxidation behaviour of monolithic TiN ceramic, Br. Ceram. Trans. J. 90 (1991) 194–196.
[8] H. Ichimura, A. Kawana, High-temperature oxidation of ion-implanted TiN and TiAlN films, J. Mater. Res. 8–5 (1993) 1093–1100.
[9] P. Lefort, J. Desmaison, M. Billy, Oxydation du nitrure de titane par l'oxygène: comportement du nitrure $TiN_{0.95}$ pulvérulent, C. R. Acad. Sci., C285 3 (1977) 361–369.
[10] P. Lefort, J. Desmaison, M. Billy, Cinétique d'oxydation du nitrure de titane: comportement de plaquettes de nitrure $TiN_{0.91}$ en atmosphère d'oxygène, J. Less-Common Met. 60 (1978) 11–24.
[11] D.J. Choi, D.B. Fischbach, W.D. Scott, Oxidation of chemically-vapor deposited silicon nitride and single-crystal silicon, J. Am. Ceram. Soc. 72 (7) (1989) 1118–1123.
[12] H. Du, R.E. Tressler, K.E. Spear, C.G. Pantano, Oxidation studies of crystalline CVD silicon nitride, J. Electrochem. Soc. 136 (5) (1989) 1527–1536.
[13] H. Du, R.E. Tresseler, K.E. Spear, Thermodynamics of the Si–N–O system and kinetic modeling of oxidation of Si_3N_4, J. Electrochem. Soc. 136 (11) (1989) 3210–3215.
[14] H. Du, R.E. Tresseler, K.E. Spear, M. Wang, Annealing studies of coupled Si_3N_4 and SiO_2 films, J. Mater. Sci. Lett. 8 (1989) 1341–1343.
[15] L.U.J.T. Ogbuji, J.M. Smialek, Evidence from transmission electron microscopy for an oxinitride layer in oxidised Si_3N_4, J. Electrochem. Soc. 138 (10) (1991) L51–L53.
[16] D.P. Butt, D. Albert, T.N. Taylor, Kinetics of thermal oxidation of silicon nitride powders, J. Am. Ceram. Soc. 79-11 (1996) 2809–2814.
[17] K.L. Luthra, A mixed interface reaction/diffusion control model for oxidation of Si_3N_4, J. Electrochem. Soc. 138 (10) (1991) 3001–3007.
[18] L.U.J.T. Ogbuji, S.R. Bryan, The SiO_2–Si_3N_4 interface, part I: nature of the interface, J. Am. Ceram. Soc. 78-5 (1995) 1272–1278.
[19] L.U.J.T. Ogbuji, The SiO_2–Si_3N_4 interface, part II: O_2 permeation and oxidation reaction, J. Am. Ceram. Soc. 78-5 (1995) 1279–1284.
[20] B.W. Sheldon, Silicon nitride oxidation based on oxinitride interlayers with graded stoichiometry, J. Am. Ceram. Soc. 79 (11) (1996) 2993–2996.
[21] M.H. Lewis, P. Barnard, Oxidation mechanism in Si–Al–O–N ceramics, J. Mater. Sci. 15 (1980) 443–448.
[22] L. Wang, C. He, J.G. Wu, Oxidation of sintered silicon nitride materials, in: Proceedings of the third International Symposium on Ceramic Materials and Components for Engines, Las Vegas, American Ceramic Society, 1988, pp. 604–611.
[23] D.R. Clarke, F.F. Lange, Oxidation of Si_3N_4 alloys: relation to phase equilibria in the system Si_3N_4–SiO_2–MgO, J. Am. Ceram. Soc. 63 (9-10) (1980) 586–593.
[24] C.O. Meara, J. Sjoberg, Transmission electron microscopy investigation of the oxidation of hot isostatically pressed silicon nitride with and without sintering aids, J. Am. Ceram. Soc. 80 (6) (1997) 1491–1500.
[25] G. Ziegler, J. Heinrich, G. Wötting, Review: relationships between processing, microstructure and properties of dense and reaction-bonded silicon nitride, J. Mater. Sci. 22 (1987) 3041–3086.
[26] Y.G. Gogotsi, F. Porz, The oxidation of particulate-reinforced Si_3N_4–TiN composites, Corros. Sci. 33 (4) (1992) 627–640.
[27] F. Peni, J. Crampon, R. Duclos, On the morphology and composition of the oxidized layer in Si_3N_4-based materials, Mater. Sci. Eng. A163 (1993) 5–7.
[28] Y.G. Gogotsi, F. Porz, G. Dransfield, Oxidation behavior of monolithic TiN and TiN dispersed in ceramic matrices, Oxid. Met. 39 (1/2) (1993) 69–91.
[29] F. Deschaux-Beaume, T. Cutard, N. Fréty, C. Levaillant, Oxidation of a Si_3N_4–TiN composite: microstructural investigation and modeling, J. Am. Ceram. Soc. 85 (7) (2002) 1860–1866.
[30] P. Kofstad, High temperature corrosion, Elsevier Applied Science Publishers LTD, 1988, pp. 289–298.
[31] G. Grathwohl, F. Thümmler, Creep of reaction-bonded silicon nitride, J. Mater. Sci. 13 (6) (1978) 1177–1186.
[32] Y.G. Gogotsi, F. Porz, V.P. Yaroshenko, Mechanical properties and oxidation behavior of Al_2O_3–AlN–TiN composites, J. Am. Ceram. Soc. 75 (8) (1992) 2251–2259.
[33] U.R. Evans, The Corrosion and Oxidation of Metals, Edward Arnold Publishers LTD, London, 1960, pp. 836–837.
[34] J. Persson, M. Nygren, The oxidation kinetics of β-Sialon ceramics, J. Eur. Ceram. Soc. 13 (1994) 467–484.